

Evidence for Holocene Marine Transgression and Shoreline Progradation Due to Barrier Development in Iskele, Bay of Izmir, Turkey

Beverly Goodman^{††*}, Eduard Reinhardt[§], Hendrik Dey^{††}, Joseph Boyce[§], Henry Schwarcz[§], Vasif Sahoglu^{††}, Hayat Erkanal^{††}, and Michal Artzy[†]

[†]Department of Maritime Civilizations
Recanati Institute for Maritime Studies
University of Haifa
Mt. Carmel, Israel 31905, Israel
goodman@research.haifa.ac.il

[§]Interuniversity Institute for Marine
Sciences–Eilat
Coral Beach, Eilat 88103, Israel

[§]School of Geography and Earth Sciences
McMaster University
1280 Main Street West
Hamilton, Ontario, L8S 4K1, Canada

^{††}American Academy in Rome
Via Angelo Masina 5
Roma 00153, Italy

^{††}Dil ve tarih Cografya Fakultesi
Department of Archaeology
Ankara University
Ankara, 06100, Turkey

ABSTRACT

GOODMAN, B.; REINHARDT, E.; DEY, H.; BOYCE, J.; SCHWARCZ, H.; SAHOGLU, V.; ERKANAL, H., and ARTZY, M., 2008. Evidence for Holocene marine transgression and shoreline progradation due to barrier development in Iskele, Bay of Izmir, Turkey. *Journal of Coastal Research*, 24(5), 1269–1280. West Palm Beach (Florida), ISSN 0749-0208.

This study addresses the paleogeographic coastal evolution of the coastal plain in the environs of Iskele, Turkey. Eight sediment cores were collected along a north–south and east–west transect and analyzed to determine whether the coastal environment had changed in the recent past. The results illustrate that the coastal environment consisted of a transgressive systems tract, ending approximately 6000 BP and represented by marine transgression, flooding of incised river channels, and marsh development, followed by a high stand systems tract. Five major environmental facies were identified: terrestrial, wetland, lagoon, foreshore, and upper shoreface. The high stand systems tract was characterized by the development of a beach-barrier consecutive series of longshore transport-derived sandbars. These sandbars contributed to the creation and eventual isolation and terrestrial infilling of nearshore lagoons and wetlands. Sea-level indicators indicate rapid sea-level rise reaching a peak approximately 6000 YBP, followed by deceleration of sea-level rise and resulting shoreline progradation. The construction of a causeway connecting Karantina Island to the mainland approximately 2400 years ago has accelerated the process of progradation east of the causeway by decreasing the wave energy. Sediment that would have previously been transported further east is now deposited in the zone immediately east of the causeway.

ADDITIONAL INDEX WORDS: *Sea level, Bay of Izmir, prograding shoreline, foraminifera, facies models.*

INTRODUCTION

Paleogeographic reconstruction of the Holocene coastline on the western coast of Turkey has been primarily limited to regions located at the mouths of major rivers (*e.g.*, BRÜCKNER, 2003; CROUCH *et al.*, 2002; KRAFT *et al.*, 2003), while less populated coastal zones away from primary rivers have been largely overlooked. In the Bay of Izmir (Figure 1), along the coastline stretching from the heavily populated city of Izmir, construction is occurring at a rapid pace. While there are smaller heavily channelized rivers, there are no major point sources for sediment contribution, yet progradation appears to have occurred. This study aims to understand and explain the processes (*e.g.*, sea level and tectonics) that have created the current coastal configuration as a means to predict changes into the future and to compare to coastlines elsewhere.

Extensive research has been done on Aegean and Mediterranean sea-level change (*e.g.*, EROL, 1981; FLEMMING, 1978; FOUACHE, SIBELLA, and DALONGEVILLE, 1999; KRAFT and RAPP, 1975; KRAFT, ASCHENBRENNER, and RAPP, 1977; KRAFT, KAYAN, and EROL, 1980; LAMBECK, 1996; LAMBECK and BARD, 2000; LAMBECK and PURCELL, 2005; LAMBECK *et al.*, 2004; PIRAZOLLI, 1994; SIVAN, ELIYAHU, and RABAN, 2004; SIVAN *et al.*, 2005; VELLA and PROVANSAL, 2000). When sea-level curves developed from sea-level markers at specific locations in the Aegean are compared (Figure 2), it becomes evident that there are considerable differences in local relative sea level, a typical and expected result in tectonically active areas. In this study, a few independent markers for local relative sea level were established and compared to previous sea-level curves to determine whether it was possible to apply a known eustatic sea-level curve or whether there were local discrepancies from previously observed norms, which would signify the presence of tectonic offsets. The most recent seismic activity in the Urla region occurred



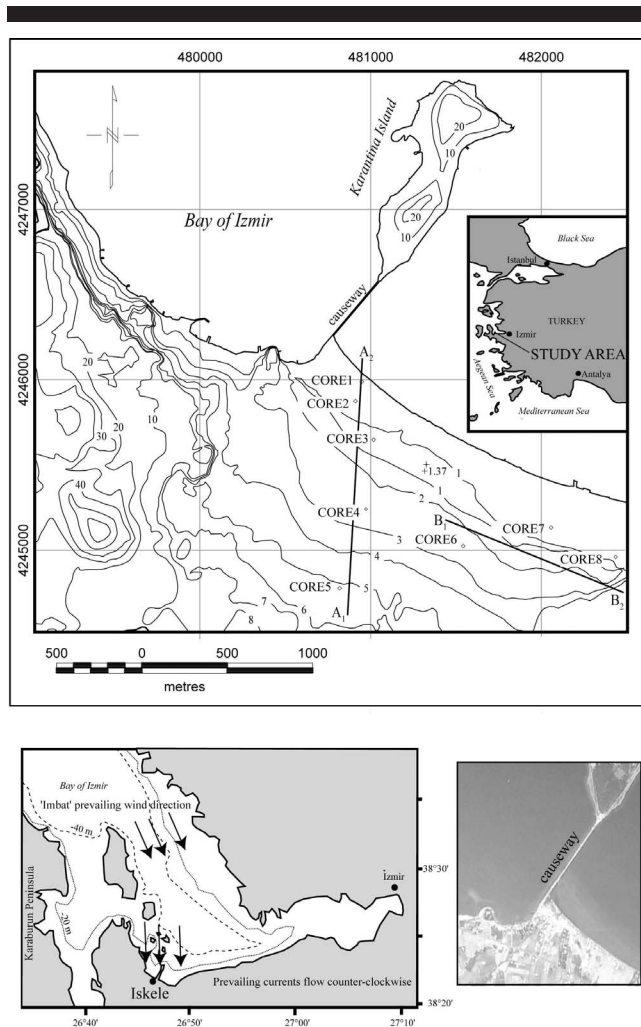


Figure 1. Maps of study area. The topographic contours on the upper map are based on a 1969 photogrammetric survey of the Urla region, and the coastline was determined during this study with DGPS. The lower map is adapted from Sayin, 2003.

October 17–20, 2005, and had maximum shock events equaling moment magnitude (M_w) 5.8 (BENETATOS *et al.*, 2006). Earthquake catalogues of the Aegean region from 500 BC to the present demonstrate regular earthquake activity, with maximum values of approximately M_w 6.5 (ALTINOK *et al.*, 2005; AMBRASEYS and FINKEL, 1990, 1991, 1995; CROUCH *et al.*, 2002; NUR and CLINE, 2000; PAPAACHOS *et al.*, 2000).

Study Area

The study area is located within the microtidal (± 15 cm) Bay of Izmir, between the modern city of Izmir and the Karaburun Peninsula (Figure 1). The bay is within the higher range of Mediterranean salinities, averaging 39.1 ± 0.51 parts per thousand (SAYIN, 2003).

The near-coastal terrestrial environment in the study area is characterized by a gradual coastal plain that meets a low-relief mountain range of volcanic origin (200 to 300 m ele-

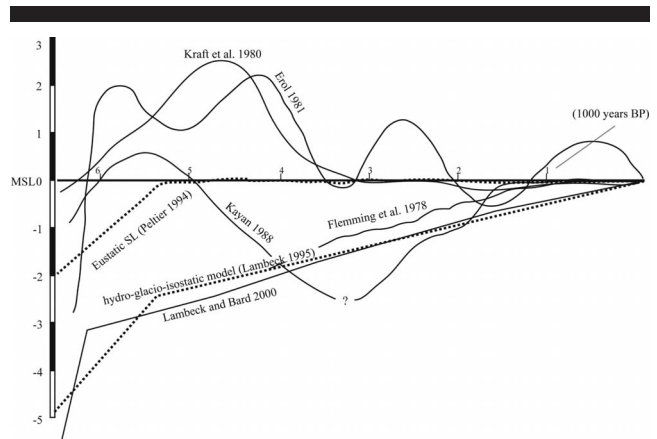


Figure 2. Sea-level curves based on data points in the Aegean (Erol, 1981; Fleming, 1978; Kayan, 1988; Kraft, Kayan, and Erol, 1980). Eustatic sea-level curves (Lambeck and Bard, 2000; Peltier, 1994).

vation) five kilometers from the coast (BRINKMANN, 1970; Figure 2). The bedrock nearer the study location consists of Neogene limestones and marls. Small, heavily channelized rivers flow from the mountains to the sea, with greater outflow in the winter months than in the summer. Precipitation ranges from 600 mm to 1300 mm, the majority of which falls between September and May. The shoreline west of the causeway to Karantina Island consists of rocky to coarse-pebble beaches with concrete walkways and small artificial seawalls designed to minimize erosion from the microtidal system and summer storms (~ 1.5 m maximum wave height). East of the causeway, the coast is characterized by a series of shallow, fine-grained lagoons (Figure 3). The bathymetry from the shoreline is gradual, reaching an approximately 15-m depth 500 m from the shore. The -40 m contour lies approximately 2 km north of the shoreline (AKSU, PIPER, and KONUK, 1987; Figure 1).

The predominant winds in the Bay of Izmir, referred to locally as “meltem” or “imbat,” flow from northwest to southeast but are predominantly from the north in the portion of the bay surrounding the study area because of the irregular distribution of landforms and sea encountered by winds approaching the area from the west (SAYIN, 2003). The resulting counterclockwise gyre produces easterly currents at the study area itself (AKYARLI, ARISOY, and ER, 1988; SANER, 1994; SAYIN, 2003; Figure 1). This is especially apparent when comparing the waters east and west of the causeway that connects Karantina Island to the mainland. While the water surface west of the bay is often choppy with whitecaps, the eastern side is mostly calm due to the interruption of wave energy by the causeway and some wind protection from the island.

METHODS

Eight sediment cores were collected using an Eijelkamp percussion corer. Coring locations were selected with the objective of producing generalized shore-perpendicular and shore-parallel cross-sections (Figure 1).

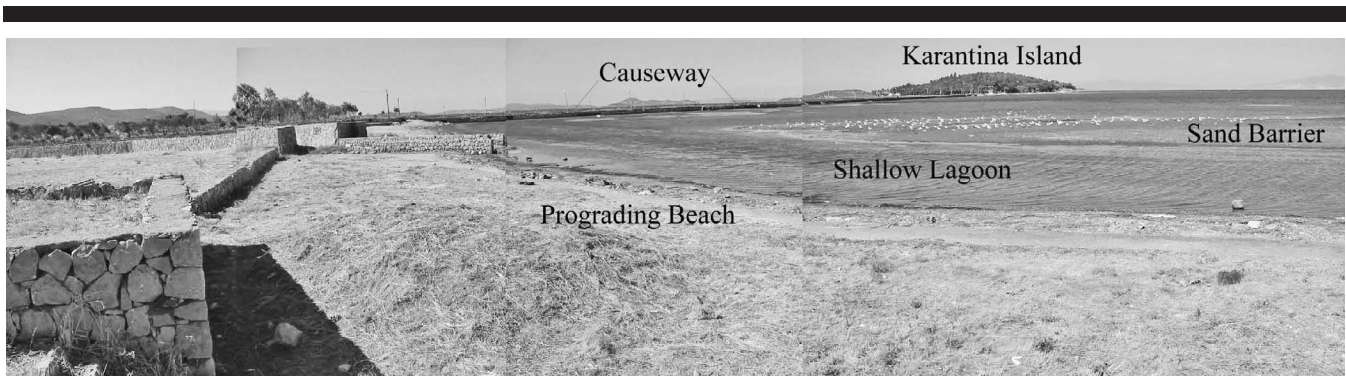


Figure 3. Photograph of the present-day prograding beach east of the causeway. For a color version of this figure, see page 1221.

Their positions and elevations were mapped using a hand-held global positioning system (GPS), Trimble differential global positioning system (DGPS), and a total station. The contours of a 1:5000 photogrammetric map were digitized and combined with coastline data points collected with the Trimble DGPS and processed using Oasis software. The specific positions of the cores were selected in the field by finding the lowest elevations to maximize penetration depth. Because of this, the core elevations and the generalized map contours do not always agree, as the map does not entirely reflect the topographic variations on the ground.

Within each core, samples were collected above and below contacts and in approximately 5 cm intervals, with allowances made for thinner horizons and extensive homogenous horizons. Sedimentological (grain size), micropaleontological, and geochemical analysis ($\delta^{18}\text{O}$ and $\delta^{13}\text{C}$) were performed at McMaster University using preparation and analysis methods given by REINHARDT, FITTON, and SCHWARCZ (2003). The precision of analyses was $\pm 0.2\text{‰}$ for both isotopes.

An aliquot of each sample was subsampled, processed with hydrogen peroxide to remove organic material, and then analyzed to determine fine-grain size using a Beckman LS Coulter Counter.

For micropaleontological analysis, the 45- to 500- μm portion of an aliquot of each sample was used for analysis. Samples with organic-walled or otherwise delicate individuals were counted wet, and the remainder were dried and floted (for methods, see FISHBEIN and PATTERSON, 1993; SCOTT and MEDIOLI, 1986). Identifications and environmental constraints of particular foraminifera and assemblages were determined based on major regional references (CIMMERMAN and LANGER, 1991; HOTTINGER *et al.*, 1993; MURRAY, 1991) and site-specific references (*e.g.*, AVSAR and ERGIN, 2001; HYAMS, ALMOGI-LABIN, and BENJAMINI, 2002; NIXON, 2001). Species not recognized in those references were described as species A, B, C, and so on. Particular dominant taxa were photographed with a scanning electron microscope at the Brockhouse Institute for Materials Research at McMaster University to assist with identification and to determine the presence or absence of diagenesis.

Each aliquot was divided and counted until a minimum of 300 specimens were identified, whenever possible (following

FISHBEIN and PATTERSON, 1993). In certain cases, fewer than 300 specimens were counted because abundance in the total sample available was lower than 300. The data were then normalized and estimated weighted maximum likelihood (EWML) was used to determine nonstatistically significant taxa and to normalize the data (see FISHBEIN and PATTERSON, 1993, for an explanation of the statistical method). Only samples with greater than 50 specimens per cubic centimeter (cc) were used to determine the foraminiferal bio-clusters, as they are statistically more reliable. Specimens with less than 1% abundance, accounting for standard error, were removed from consideration when determining biofacies. Error-adjusted data (normalized) for samples with abundance greater than 50 per cc were then processed using the statistical package PAST (HAMMER, HARPER, and RYAN, 2001) to produce Ward-method clusters of related assemblages and samples. Samples with lower abundance (below 10 per cc) were reviewed for resemblance to the established clusters to assist with determining their facies designations.

$\delta^{18}\text{O}$ and $\delta^{13}\text{C}$ values (for preparation and analysis methods, see REINHARDT, FITTON, and SCHWARCZ, 2003) were determined for select species chosen to represent a wide range of environmental tolerances, such as *Ammonia*, in order to track isotopic values through the entire extent of the core and minimizing the influence of interspecies-specific vital effects. When one species was not present throughout all horizons, comparisons of all samples in each horizon analyzed could then be compared to determine the presence of trends.

Underwater surface samples were collected to establish the present $\delta^{18}\text{O}$ and $\delta^{13}\text{C}$ values for comparison. The freshwater meteoric precipitation endmember $\delta^{18}\text{O}$ value (approximately -5.0‰) was determined with the use of Global Network of Isotopes in Precipitation (GNIP) data from the International Atomic Energy Agency (IAEA). With the use of the modern marine and freshwater $\delta^{18}\text{O}$ endmembers, salinity categories from freshwater to fully marine water were established. Generally, values equal to $1.5\text{‰} \pm 1$ were considered typical marine; figures greater than this value represent evaporative brackish or marine, and lower values were anticipated in brackish and freshwater environments.

Radiocarbon dating was used to provide chronological constraints on the facies transitions (Table 1). Organic material

Table 1. Radiocarbon dates. All samples were processed using AMS method. The plant materials were indistinguishable from broken-down plant material.

Core	Depth (msl)	C14 Date (YBP)	Corrected C14 Date (Terrestrial)	95.5% Confidence Interval	C14 Date (Marine)	95.5% Confidence Interval	$\delta^{13}\text{C}/\delta^{12}\text{C}$ (‰)	Dated Material	Laboratory Number
8	-1.9	2770 ± 40	2800 ± 40	2980–2790	N/A	N/A	-23.2	Peat	Beta-194729
7	-3.26	4080 ± 40	4260 ± 40	4860–4820 and 4750–4720	N/A	N/A	-14.3	Peat	Beta-194730
7	-1.85	2700 ± 40	2870 ± 40	3090–2870	N/A	N/A	-14.3	Peat	Beta-194731
8	-4.35	4370 ± 40		5250–4960	4410	4550–4270	1.9	Marine shell	Beta-194732
4	-0.59	4370 ± 40		5240–4950	4400	4545–4255	1.1	Marine shell	Beta-191877

mssl = mean sea level.

within the cores (shell, plant matter) was separated for radiocarbon analysis. The ages of five samples were processed using approximate mode-superposition (AMS) technique at the Beta-Analytic Laboratory.

Separate facies (biofacies, lithofacies, envirofacies) were determined based on the micropaleontological, sedimentological, geochemical, and chronological data (see the example core in Figure 4). Correlation between horizons was determined by the similarity between these facies or succession of facies. In certain cases multiple facies were continuous across nearby cores, and in others disconformities were present.

Sediment cores were examined for dateable sea-level markers such as peat and foraminifera–thecamoebian transitions. In particular, dateable horizons in which there was an indication of a transition from marine-derived sediments to fresh-

water or terrestrial sediments, based on the proxies, were selected. Markers with a known relative position to sea level were in turn plotted on a graph with supratidal, subtidal, and intertidal designations and then compared to previously established sea-level curves (Figure 5).

RESULTS

Facies

Five major environmental facies were determined based on the results of the multiproxy analysis. They included terrestrial, wetland, foreshore, lagoon, and upper shoreface (Tables 2 and 3, Figures 6 and 7).

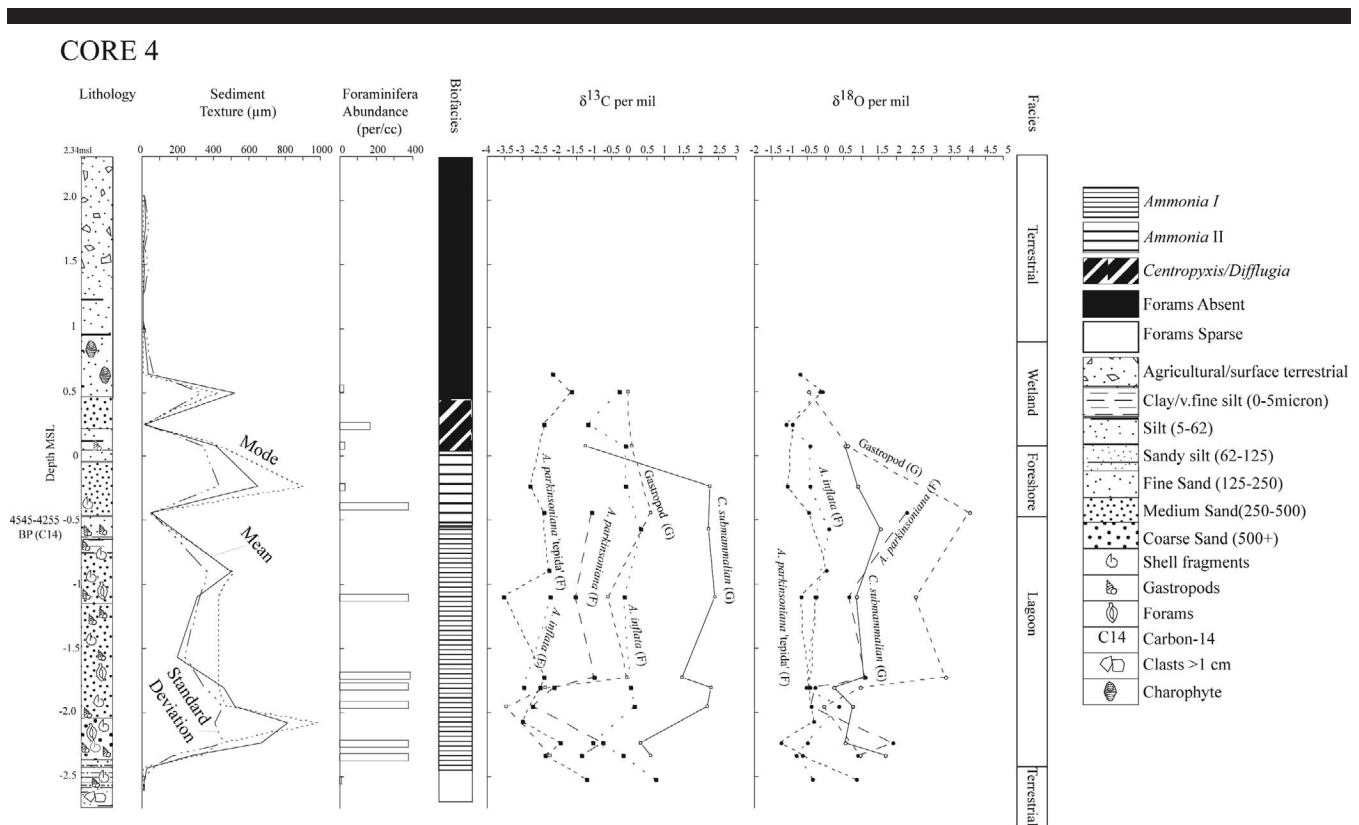


Figure 4. Sample of a detailed analyzed core used for correlating and determining facies.

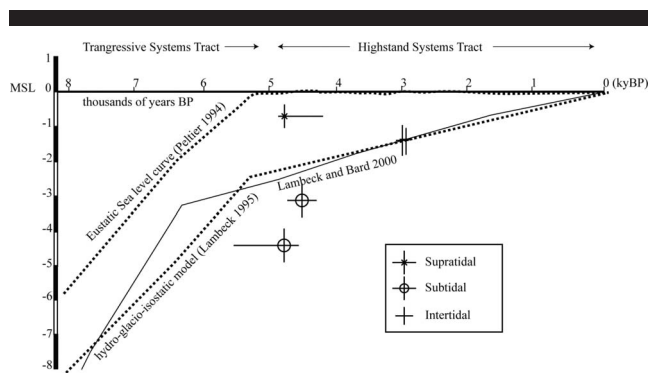


Figure 5. Radiocarbon-dated samples and relative sea-level positions (refer to Table 2 for reference data).

Terrestrial

The terrestrial facies was defined by an absence or low abundance (an average of less than two specimens per cc) of foraminifera, silt-range average grain size, and in most cases, continuity with the modern surface (Tables 2 and 3). Abun-

dances were lower than the minimum necessary to be included in the biofacies analysis, which is limited to samples with more than 50 specimens per cc. When present, foraminifera were heavily eroded or broken, an indication of transport or dissolution. These foraminifera may have been deposited during higher magnitude storm run up or as a result of heavy winds. The color of the sediment ranged from yellow–brown to within the gray spectrum. The characteristics of modern surface terrestrial samples (based on the topmost, indisputably terrestrial sediment layer of cores) were used as a reference for samples collected beneath the modern surface (Figures 6 and 7).

Wetland

The wetland facies is characterized by coarse silt–sized average grain-size values, biofacies clustering into the *Centropyxis/Difflugia* and *Trochammina* biofacies groups, low to medium diversity, isotope values depleted relative to modern marine values, and light gray to yellow–brown sediments (Tables 2 and 3). The wetland facies occurs in two types, freshwater and brackish.

The freshwater wetland facies horizons are represented by

Table 2. Average abundances per cluster group. Data based on samples with greater than 50 specimens counted and species represented in abundances greater than 1% in at least one sample (for methods, see Fishbein and Patterson, 1993). Clustering was completed with PAST micropaleontological statistical package software (Hammer, Harper, and Ryan, 2001).

Biofacies Cluster Name:	<i>Centropyxis/Difflugia</i>			<i>Ammonia</i>		<i>Elphidium</i>	
	<i>Trochammina</i>	<i>Haynesina</i>	I	II	I	II	
Facies Interpretation:	Wetland			Lagoon		Upper Shoreface/Foreshore	
Salinity Interpretation:	Freshwater	Brackish	Marine–Hypersaline	Brackish–Marine	Brackish–Marine	Marine	Marine
No. samples included:	2	4	3	9	7	7	13
Avg. forams per cc:	293 ± 40	221 ± 139	670 ± 435	458 ± 135	86 ± 14	194 ± 77	324 ± 178
Avg. taxa per sample:	7 ± 4	3 ± 1	7 ± 1	12 ± 3	23 ± 15	43 ± 10	41 ± 15
Avg. Shannon diversity (H):	1.24	0.18	0.80	0.89	1.38	2.91	3.04
<i>Ammonia inflata</i> †	—	—	—	0.2 ± 0.1	24.9 ± 28.0	2.7 ± 2.8	1.3 ± 4.2
<i>A. mamilla</i>	—	—	—	—	0.4 ± 0.6	2.9 ± 1.4	2.9 ± 2.5
<i>A. parkinsoniana</i>	0.8 ± 1.1	—	1.1 ± 0.8	3.7 ± 7.1	—	7.3 ± 3.9	2.1 ± 2.6
<i>A. tepida</i>	1.1 ± 1.5	0.1 ± 0.3	0.4 ± 0.4	75.6 ± 9.7	0.5 ± 0.9	0.1 ± 0.3	9.8 ± 8.6
<i>Ammonia</i> sp. A	—	—	—	—	39.7 ± 15.8	8.0 ± 4.1	0.9 ± 3.2
<i>Centropyxis aculeata</i>	42.7 ± 11.4	—	—	—	—	—	0.2 ± 0.7
<i>C. constricta-silica</i>	27.3 ± 11.2	—	—	—	—	—	—
<i>Cibicides refulgens</i>	—	—	—	—	0.2 ± 0.6	3.5 ± 2.3	4.3 ± 2.5
<i>Difflugia oblonga</i>	25.5 ± 3.0	—	—	—	—	—	—
<i>Elphidium advenum</i>	0.2 ± 0.2	—	—	—	0.9 ± 1.1	11.0 ± 6.1	2.7 ± 2.0
<i>E. macellum</i>	0.2 ± 0.2	—	—	0.0 ± 0.1	1.3 ± 1.3	7.3 ± 2.1	6.9 ± 4.8
<i>Eponides</i> sp. A	—	—	—	—	0.2 ± 0.4	3.7 ± 3.9	4.5 ± 2.6
<i>Gyroidinoides</i> sp. A	—	—	—	3.8 ± 2.2	3.1 ± 3.9	—	0.1 ± 0.4
<i>Haynesina depressula</i>	—	—	9.6 ± 6.1	0.9 ± 2.6	—	0.8 ± 2.1	3.5 ± 2.8
<i>Haynesina</i> sp. D	—	—	78.0 ± 9.9	—	—	—	—
<i>Planorbulina mediterraneensis</i>	—	—	0.1 ± 0.2	—	—	2.4 ± 2.8	1.4 ± 3.3
<i>Peneroplis pertusus</i>	—	—	—	—	—	2.5 ± 2.8	—
<i>Quinqueloculina</i> sp. A	—	—	—	—	—	2.2 ± 3.2	0.1 ± 0.3
<i>Rosalina bradyi</i>	—	0.1 ± 0.1	—	—	0.7 ± 1.2	3.8 ± 2.5	6.8 ± 6.0
<i>Trochammina macracens</i>	—	—	—	1.6 ± 3.7	—	—	1.8 ± 4.2
<i>Triloculina subgranosum</i>	—	—	—	8.0 ± 4.5	4.0 ± 5.0	0.3 ± 0.8	—
<i>Trochammina</i> sp. A	0.8 ± 1.1	94.4 ± 8.1	—	—	—	—	2.0 ± 6.4
<i>T. inflata</i>	—	4.3 ± 8.5	—	1.2 ± 3.1	—	—	2.8 ± 5.9
Total % represented	98.4	98.9	89.2	94.9	75.8	58.5	53.8

† Average abundances are given as percentages ± 1 sigma (standard error).

Table 3. General descriptions of facies characteristics. Grain size based on Udden-Wentworth grain-size classification scheme (Wentworth, 1922). Shannon diversity index, low = 0–1.0, medium = 1.0–2.0, and high = 2.0–3.0.

Facies	Modal Grain Size	Sediment Color	Biofacies Clusters	Biodiversity	$\delta^{13}\text{C}$ (‰VPDB)	$\delta^{18}\text{O}$ (‰VPDB)
Terrestrial	Silt	Various	Absent or very low abundance	N/A	N/A	-5.0 [†]
Wetland	Coarse silt	Light gray to yellow-brown	Absent or low abundance, <i>Centropyxis/Difflugia</i> , and <i>Trochammina</i>	Low–medium	-0.3 ± 1.2	-0.4 ± 1.0
Foreshore	Coarse sand	Various	Low abundance, <i>Elphidium</i> I and II	Medium–high	0.5 ± 1.3	0.3 ± 0.6
Lagoon	Fine sand	Very dark gray	<i>Ammonia</i> I and II, <i>Haynesina</i>	Low–medium	-0.9 ± 2.2	0.6 ± 1.1
Upper shoreface	Medium sand	Gray to very dark gray	<i>Elphidium</i> I and II	High	0.5 ± 2.9	0.6 ± 1.7

VPDB = Vienna Peedee belemnite.

[†] Value based on GNI.

biofacies *Centropyxis/Difflugia*; samples dominated by *Centropyxis aculeata* (42.7% ± 11.4), *C. constricta-silica* (27.3% ± 11.2), and *Difflugia oblonga* (25.5% ± 3.0). *C. constricta-silica* and *Difflugia* are common, slightly brackish to freshwater species (Figures 6 and 7). They represent the presence of freshwater contribution from precipitation, groundwater, and/or alluvial input. Average grain-size values (micrometers) are mean 25 ± 12, median 6 ± 0, mode 6 ± 1, and standard deviation 41 ± 25. These silt-size values are consistent with a low-energy environment, such as that of a wetland marsh. In some cases, megaspores and charophytes are present within the wetland freshwater facies horizons and at the contact between the wetland brackish and the wetland freshwater facies. Charophytes are a proxy for freshwater to slightly brackish still water, and megaspores are a proxy for the presence of tall grasses and rushes common on the borders of freshwater and brackish wetlands (BRASIER, 1980; CURREY, 1966; FIEST-CASTEL, 1977; SOULIE-MARSCHÉ, 1991; ZATON, PIECHOTA, and SIENKIEWICZ, 2005). The average isotopic values of the freshwater wetland facies (see core 4, Figure 4, for individual species values) are $\delta^{18}\text{O} = -0.1\text{‰}$ and average $\delta^{13}\text{C} = -0.9\text{‰}$. The values are slightly depleted relative to full marine values. These values indicate either that the thecamoebians have been transported from a freshwater system or that the foraminifera analyzed were transported. Alternatively, this could reflect seasonal changes and fluctuations that produce blooms of different taxa at different times of the year. During the driest portion of the year, evaporation results in higher salinities that are hospitable to marine taxa, while the wetter winter months result in lower salinities preferred by thecamoebian taxa.

The brackish wetland environment is represented by the *Trochammina* biofacies. *Trochammina* sp. A is present at values greater than 90% and is copresent with *T. inflata* (Table 2). While some species of *Trochammina* are fully marine and occur in deep water, the *Trochammina* sp. present here prefer silty, organic-rich environments; tolerate a variety of salinity regimes; and are particularly capable of handling fluctuating salinities often found in marine marshes. Grain-size values are represented by a large range from silty to sandy, with the sandy proportions situated at the onset and closing of the horizons. The values are mean 262 ± 388, median 243 ± 434, mode 399 ± 562, and standard deviation 196 ± 228. The low sorting values are characteristic of environments

with multiple transport processes, of the sort expected for brackish wetlands (Figures 6 and 7).

The average isotopic values of the wetland brackish facies are $\delta^{18}\text{O} = 0.3\text{‰}$ and $\delta^{13}\text{C} = 0.5\text{‰}$. The $\delta^{18}\text{O}$ values are slightly depleted relative to marine water, indicating freshwater mixing, and the $\delta^{13}\text{C}$ value is close to marine values. This suggests that freshwater was being deposited from runoff and/or precipitation and that evaporation led to increased, or more near-marine water relative to full freshwater, $\delta^{18}\text{O}$ values.

Lagoon

The lagoon facies is characterized by the biofacies *Haynesina* and *Ammonia* I and II; average mode grain-size values in the very fine sand range; very dark gray sediments; oxygen isotope values near marine values ($\delta^{18}\text{O} = 0.6 \pm 1.1\text{‰}$); carbon isotope values depleted with respect to marine values ($\delta^{13}\text{C} = -0.9 \pm 2.2$); and low biodiversity (Tables 2 and 3).

Ammonia I is distinguished by the heavy dominance of *A. tepida* (75%) and the presence of *Trochammina* spp. The copresence of these taxa is common in nearshore brackish environments (AMOROSI *et al.*, 1999; FIORINI, 2004; SCOTT, SCHAFER, and MEDIOLI, 2001). The *Ammonia* II biofacies is distinguished by 39% *A. parkinsoniana* sp. A, 24% *A. inflata*, and near-equal abundances (~3%) of *Triloculina subgranosum*, *Gyroidinoids* sp. A, and *A. parkinsoniana*. Unlike *Ammonia* I, *Ammonia* II is more characteristic of normal marine conditions, with greater diversity, but it lacks abundances typical of normal marine. Overall, the biofacies of *Ammonia* I and *Ammonia* II typical of brackish–marine lagoons contain euryhaline living brackish and hypersaline species (Figures 6 and 7).

The *Haynesina* biofacies, characterized by low diversity and the dominant presence of *H. depressula* and *Haynesina* sp. D, is more typical of a hypersaline lagoon complex (AMOROSI *et al.*, 1999; HAYWARD *et al.*, 2004; VANICEK *et al.*, 2000). The proportional abundance in the biofacies is 78% *Haynesina* spp. and 9.6% *H. depressula*. Diversity is typically low in these samples, and abundance is lower than in a normal marine biofacies, both typical characteristics of hypersaline assemblage zones (SCOTT and MEDIOLI, 1986). *Haynesina* is also found in marine environments and can be an efficient

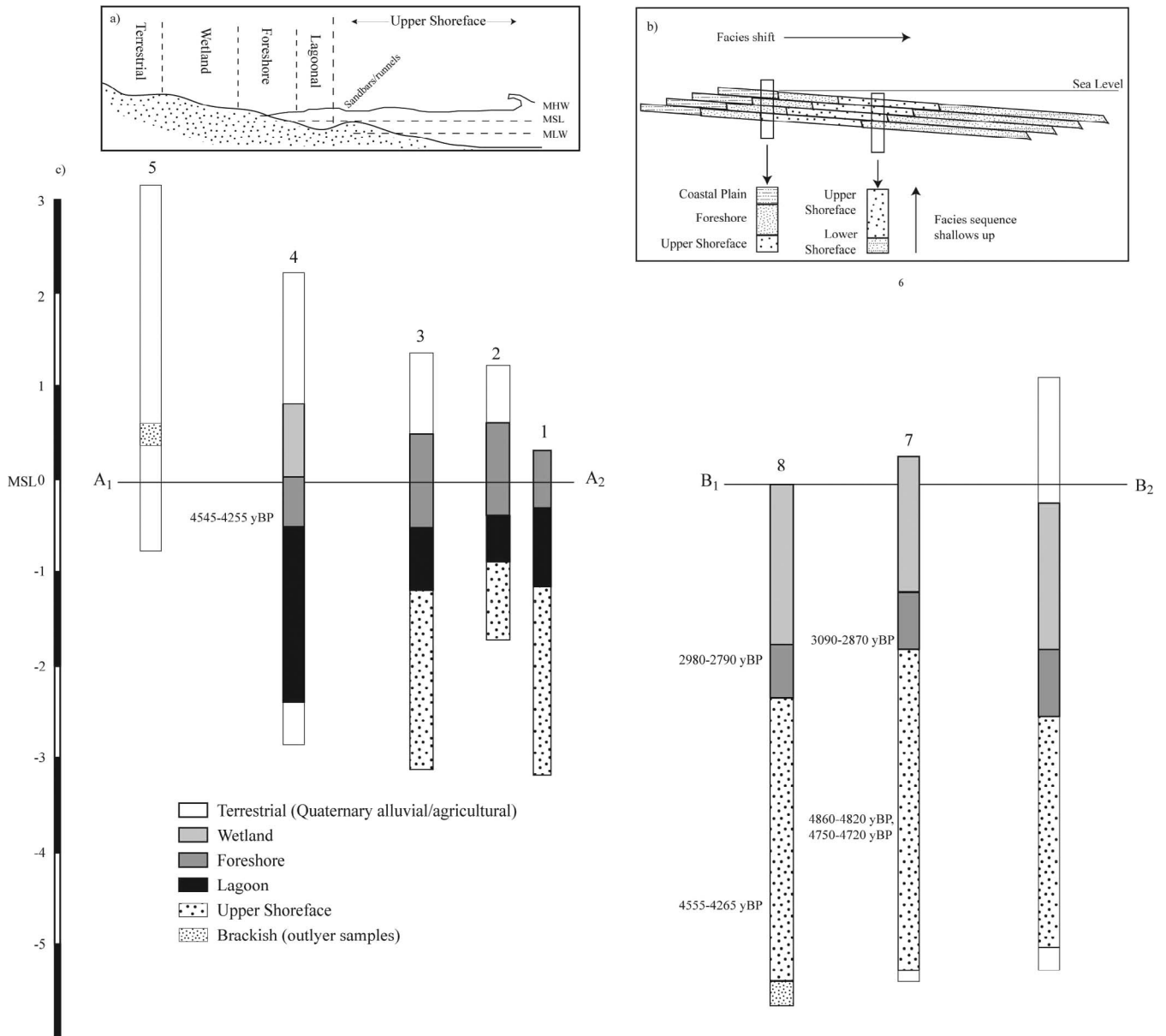


Figure 6. (a) Generalized cross-section profile of facies positions. (b) Generalized regressive systems tract (adapted from Nichols, 1999). (c) Transect A and transect B cores with facies horizons indicated. Refer to Figure 2 for map of transect positions.

colonizer of lagoonal environments in the littoral zone (SCOTT and MEDIOLI, 1986).

Upper Shoreface

The upper shoreface facies is characterized by samples that clustered into biofacies *Elphidium* I and II, gray to dark gray sediment with modal grain-size values averaging in the medium sand range, and high biodiversity (Tables 2 and 3).

Elphidium I and II consist of high-diversity samples containing shoreface-preferring taxa. The *Elphidium* I and II biofacies have a greater than 10% presence of *Elphidium* (*E. advenum*, *E. jenseni*, *E. macellum*, *E. translucens*), along with

the presence of *A. parkinsoniana*. *E. advenum* and *E. macellum* were the most abundant of the *Elphidium* sp. present; however, there were up to 18 different *Elphidium* sp. in an individual sample, in some cases greater than 50% *Elphidium* abundance in a single sample. In general, *Elphidium* has been used as an indicator of marine conditions (salinity, turbidity, substrate). *Elphidium* is present in sample locations nearest to the mouths of estuaries in water closest to marine values (*E. crispum*, *E. williamsoni*; RUIZ *et al.*, 2005). CANN *et al.*'s (2002) Port Pirie, Australia, study identified *Elphidium* in the subtidal and intertidal horizons (*E. crispum*, *E. advenum*). In the Aegean, AVSAR and ERGIN (2001)

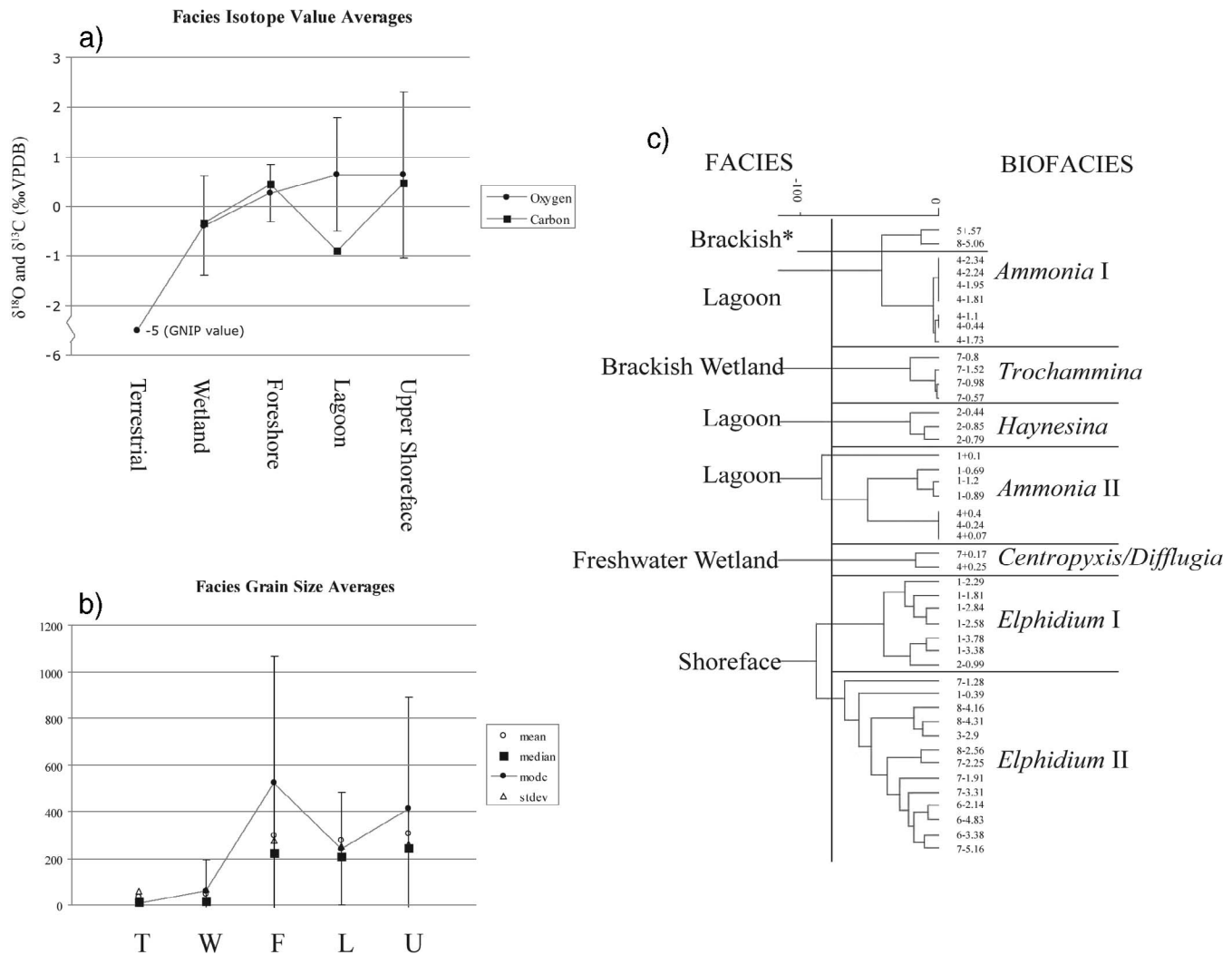


Figure 7. Facies relationships: (a) average isotope values, (b) grain-size values, (c) Ward's method clusters based on foraminifera (see Table 2 for details). Upper two samples represent unusual outliers. They are present in two very different environments, which seem to represent a brief event that relates to an intrusion of freshwater that then is evaporated or mixed with marine water. In the case of the sample core 8/-5.06, the event occurs just at the beginning of the marine incursion, indicating the possible meeting of the shoreline to a small river outlet (marked estuary on the top plan reconstruction), and in the case of core 5/+0.57, it is likely the result of a temporary freshwater pool that during its evaporative phase was saline enough to support a bloom of foraminifera.

established that *Elphidium* was present in the nearshore shallow facies (*E. advenum*, *E. crispum*, *E. macellum*). *E. crispum* and *E. advenum* were also common species in the nearshore environments of the coast of Egypt (SAMIR *et al.*, 2003).

All upper shoreface facies sample grain-size averages range from fine to coarse sands with large standard deviations indicating poor sorting. At Iskele, this variation may be the result of the combined influences of wave energy, sea grasses (sediment trapping), and anthropogenic factors (GACIA and DUARTE, 2001).

No *Elphidium* I samples were analyzed for isotopic values. *Elphidium* II biofacies had isotopic averages of $\delta^{18}\text{O} = 0.6$ and $\delta^{13}\text{C} = 0.6\text{‰}$ (Figure 7).

Foreshore

The foreshore facies is distinguished by a low abundance (absent or fewer than 25 per cc) of microfossils, average modal grain-size values in the coarse-sand range, varied sediment coloring, and isotope values $\delta^{18}\text{O} = 0.3\text{‰} \pm 0.6$ and $\delta^{13}\text{C} = 0.5\text{‰} \pm 1.3$ (Tables 2 and 3, Figures 6 and 7). These values are slightly depleted but within the range of marine values. Grain size of the foreshore facies is the most indicative characteristic.

Brackish-Evaporative Outlier Samples

Two samples (core 8/-5.06 msl, core 5/+0.57 msl) clustered in tandem within the lagoonal facies biocluster, but the re-

maining characteristics of the samples do not coincide with that interpretation. With exception to their micropaleontological character, the two samples are entirely different from the remaining lagoonal samples but similar to each other because they include high proportions of *A. tepida* copresent with smaller proportions of *H. depressula*.

DISCUSSION

The results obtained from analysis of the Iskele cores illustrate a coastal environment beach-barrier sequence that begins with marine transgression and evolves into the present coastline. The earliest sequence visible in transect A, which runs shore perpendicular and consists of upper shoreface horizons copresent with a lagoon (Figure 6). The sea transgression reached at least 700 m inland relative to the modern coastline by 4545–4255 (1σ) based on the sample dated from the foreshore–lagoon contact (core 4/–0.57 msl). A bounding disconformity with a ravinement surface is visible at the base of core 4 (particle size and more than 1 cm gravel) at the terrestrial and lagoon contact. The transition from shoreface to lagoon to foreshore, visible in cores 1, 2, and 3, paired with the wetland horizon in core 4, represents the facies changes resulting from shoreline progradation as the sediment budget exceeded the accommodation space and caused seaward coastline development. The isolated brackish–evaporative sample in core 5 is most likely the result of an ephemeral evaporative pool that was present long enough to support a bloom of foraminifera. Colonization of inland pools by foraminifera is made possible by the movement of birds from the sea or marshes to inland water bodies (SCOTT and MEDIOLI, 1978). The general trend of facies is indicative of a regressive systems tract (NICHOLS, 1999).

Cores 6, 7, and 8 lie on a generalized transect (transect B) nearly shore parallel east of transect A. There, the lower bounding disconformity is demarcated by the presence of a ravinement surface and an increase in grain size at the terrestrial–upper shoreface contact. The overall sequence transitions from shoreface to foreshore to wetland deposits. Core 8's lowest horizon includes a sample from the brackish–evaporative outliers, indicating some short-lived event that introduced greater amounts of freshwater into the system. This may be an indication of minor river input at that portion of the basin. The shoreface facies is present from prior to approximately 4800 YBP (see dates on Figure 6); then transitions to foreshore facies, which convert entirely to wetland approximately 2900 YBP; and ultimately become terrestrial. The system most closely resembles a transgressive systems tract followed by a high stand systems tract in which the coastal progradation is primarily the result of longshore transport. The cores represent a coastal sequence, which includes minor alluvial influence (no major sediment point source), and a sequence of brackish to marine phases, which document the replacement of sea-level transgression by shoreline progradation following the deceleration of sea-level rise (Figure 8). It resembles the model put forth by HARRIS *et al.*, 2002 (based on DALRYMPLE, ZAITLIN, and BOYD, 1992) to illustrate the transition from transgressive to prograding coastline on a mostly linear coastline with greater relative

strength in wave energy than in tidal energy. The few dated markers, when compared to the sea-level curves, are mostly in agreement with LAMBECK (1996) and LAMBECK and BARD's (2000) sea-level curves, suggesting that tectonic activity in the area has not caused any major coastal offsets. However, given the low resolution of the data *vis-à-vis* chronology and sea-level indicators, additional research will be necessary to negate the possibility of tectonic influence on the coastal geomorphology of the region.

In summary, on this coastline, a transgressive systems tract ended approximately 6000 BP and was followed by a progradational high stand systems tract. The high stand elevation is marked by the maximum incursion of seawater inland prior to the onset of coastal progradation. Sea level rose relatively rapidly following the Last Glacial Maximum, nearly reaching modern sea level around 6000 BP, and then gradually rose until it reached today's sea level. Initially, the rise in sea level created a ravinement or lag surface, which is identifiable by a spike in grain-size values in the initial marine flooding phase (visible in the deepest cores). The initial rapid sea-level rise also caused erosion at the newly established shoreline, as well as in its path, as it overtook the landmass and infilled shallow river valleys. Sea-level rise slowed, and the high stand systems tract began. At Iskele, the transition to the high stand systems tract, resulting from the slowing of sea-level rise, is represented by a regressive depositional environment, or prograding beach. This is visible in a vertical section by the presence of beach deposits (foreshore) above upper shoreface deposits as the sequence of facies migrated seaward with the buildup of shoreface. The source material for this was likely carried along the dominating westerly currents, which resulted in shore-parallel sandbars that contributed to the shallowing regressive sequence, quickening the isolation of portions of the tract and producing shallow lagoons prior to the full transition to a supratidal and finally terrestrial environment.

Similar shoreface systems have been studied worldwide, although primarily from regions outside of the Mediterranean. Deceleration of sea-level rise approximately 6000 BP is identified in many sites, where it led to transgressive shorelines, some of which are also beach-ridge systems resembling the system present in the study area. Within the Mediterranean, prograding shorelines during the recent Holocene are common, although the majority of studies have focused on areas with considerable alluvial input point sources and therefore progradation rates as high as 1 km per 1000 years (1 m/y; BRÜCKNER, 2003; KRAFT *et al.*, 2003; VÖTT *et al.*, 2006). On the coast of Nayarit, Mexico, Holocene lagoon and marsh phases were replaced by transgressive littoral sand in a regressive sequence that built the coast seaward at a rate of about 3 m/y (CURRAY, EMMEL, and CRAMPTON, 1969; WALKER and PLINT, 1992). This seaward progress of the coast in this study area was considerably slower, totaling approximately 1 km of shoreline progradation over 4000–6000 years, or an average between approximately 25 cm/y and 16 cm/y.

On the southern Australian coast (SHORT, 1988), a small proportion of sites studied (~4%) consisted of beach-ridge plain systems. There, they are present along gulfs and more

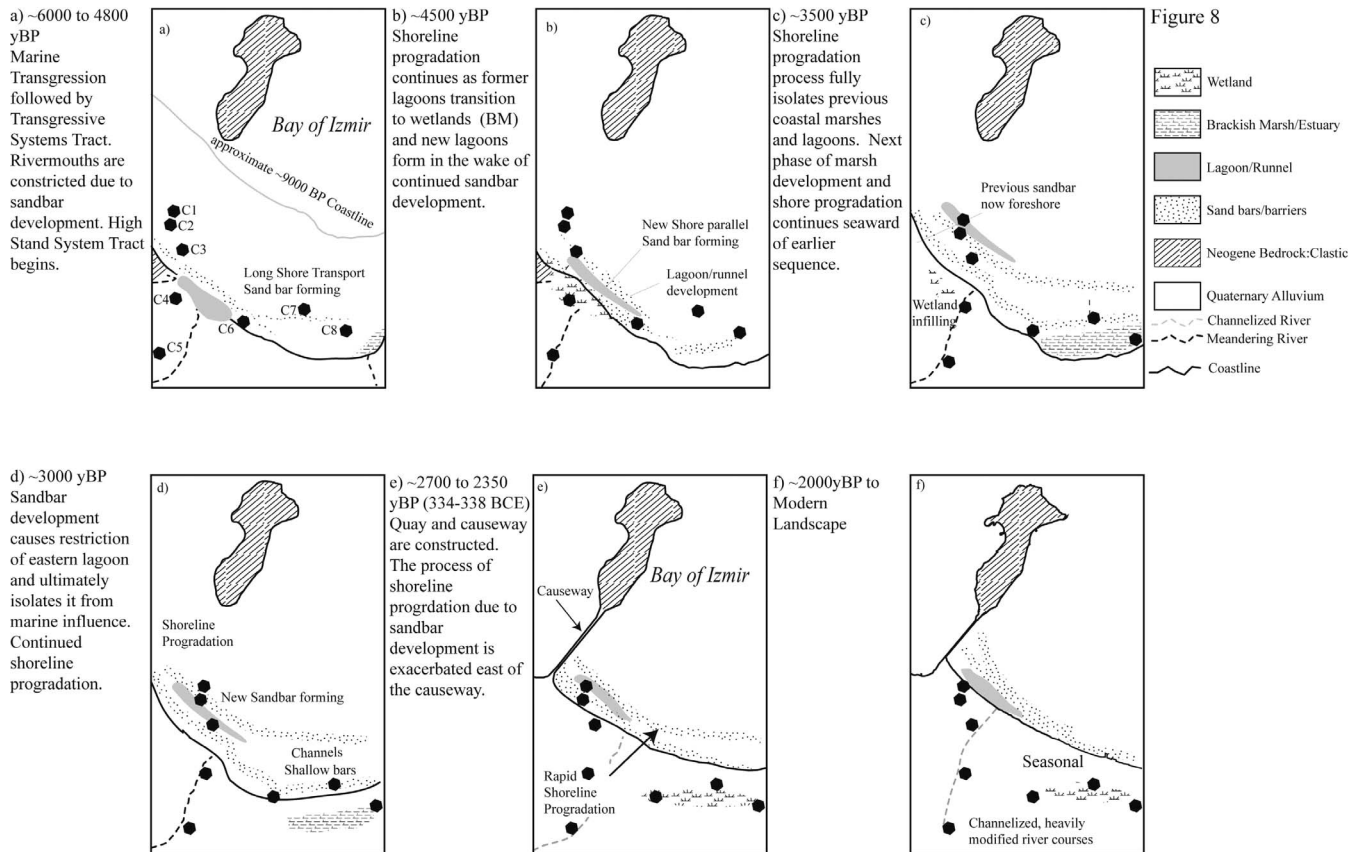


Figure 8. Paleogeographic reconstruction.

protected sections of open coast similar to the area of this study. The estimate for sea-level still stand in Australia is approximately 6500 BP. The beach-ridge plain sites of Spencer Gulf have prograded on average 700 m since the sea-level still stand and have long intertidal flats (1700 m). A macro-tidal barrier system in northwestern Australia (LESSA and MASSELINK, 2006) was similarly recognized to cause shoreline progradation following sea-level rise deceleration.

Another recent study in the Gulf of Lion (TESSON, LABAUNE, and GENSOUS, 2005) documents a similar area of coastal progradation without significant local alluvial contribution, where a majority of the sediment is provided by longshore transport. The Gulf of Lion study area was characterized by a beach-barrier depositional system in which the coastline prograded 1 km over the past 4000–6000 years, a rate similar to that recognized in this study.

The process of coastal sedimentation and progradation in the Iskele study area is especially interesting given the lack of a distinct sediment point source, as is present in comparative sites in the eastern Mediterranean (BRÜCKNER, 2003; KRAFT *et al.*, 2003; VÖTT *et al.*, 2006). While progradation at Iskele is comparatively slower (1 km per 5000 years *vs.* 1 km per 1000 years), it still occurs. Human occupation sites have been present along this coastline from as early as the Late Chalcolithic, approximately 5500 YBP (ERKANAL, 1995), and

have continuously occupied the area until the present. Sediment runoff as a result of agriculture, deforestation, and construction may have provided some of the sediment that contributed to the process of progradation. The process of progradation also appears to have been accelerated by the presence of the causeway connecting the island to the mainland, whose construction has commonly been traditionally attributed to Alexander the Great's conquest of the region in 338–334 BC (HEISSERER, 1980). Prior to the causeway, the process of longshore transport and beach-barrier development built the coastline seaward. The construction of the causeway further promoted the process of siltation and constriction by interrupting wave energy from the east, thus slowing the movement of sediment by way of longshore transport. The accelerated progradation rate caused by the causeway accounts for the divergence between the coastlines on both sides of it. The sediment budget (erosion *vs.* deposition) west of the causeway is more balanced, while the sediment budget east of the causeway is positive, resulting in the formation of sandbars and lagoons and thus ultimately in increased shoreline progradation.

CONCLUSION

This study demonstrates that the character of the coastline in the environs of Iskele has changed significantly during the

Holocene. Following the high sea-level stand approximately 6500 YBP, there were extensive lagoons and wetlands that over time became infilled and ultimately terrestrial. Although tectonic activity is present, this study has not indicated any substantial offsets or impacts from these episodes. Seismic activity may be expressed primarily in subsidence or possibly in localized offsets not recognized in the resolution of this study. The overall process of shoreline progradation in the past continues in the modern setting and is anticipated to continue as long as present conditions remain constant.

ACKNOWLEDGMENTS

In addition to individual institute support, support was provided by the Geological Society of America (B.G.), Fulbright Institute (B.G.), Hatter Foundation (M.A.), and an anonymous donor. A special thank you to all of the students and volunteers who participated in sample collections and the Joint University of Haifa and Izmir Region Excavations and Research Project archaeological excavations for collaboration and logistical support. We thank Martin Knyf for assistance in isotopic analyses and Steve Koprach for assistance in simultaneously extracted metal analyses of foraminifera.

LITERATURE CITED

- AKSU, A.E.; PIPER, D.J.W., and KONUK, T., 1987. Late Quaternary tectonic and sedimentary history of outer Izmir and Candarli Bays, Western Turkey. *Marine Geology*, 76, 89–104.
- AKYARLI, A.; ARISOY, A., and ER, T., 1988. Current and sea-level measurements performed in the Izmir Bay. Proceedings of the Environmental Science and Technology Conference (Izmir, Turkey). *Environment*, 1, 1–12.
- ALTINOK, Y.; ALPAR, B.; ÖZER, N., and GAZIOGLU, C., 2005. 1881 and 1949 earthquakes at the Chios-Cesme Strait (Aegean Sea) and their relation to tsunamis. *Natural Hazards and Earth System Sciences*, 5, 717–725.
- AMBRASEYS, N.N. and FINKEL, C.F., 1990. The Marmara sea earthquake of 1509. *Terra Nova*, 2, 167–174.
- AMBRASEYS, N.N. and FINKEL, C.F., 1991. Long-term seismicity of Istanbul and the Marmara sea region. *Terra Nova*, 3, 527–539.
- AMBRASEYS, N.N. and FINKEL, C.F., 1995. *The Seismicity of Turkey and Adjacent Areas: A Historical Review, 1500–1800*. Istanbul: Muhihin Salih EREN.
- AMOROSI, A.; COLALONGO, M.L.; PASINI, G., and PRETI, D., 1999. Sedimentary response to Late Quaternary sea-level changes in the Romagna coastal plain, northern Italy. *Sedimentology*, 46, 99–121.
- AVSAR, N. and ERGIN, M., 2001. Spatial distribution of Holocene benthic foraminifera, northeastern Aegean Sea. *International Geology Review*, 43, 754–770.
- BENETATOS, C.; ROUMELIOTI, Z.; KIRATI, A.; GANAS, A.; ZIAZIA, M.; PLESSA, A., and DRAKATOS, G., 2006. Properties of the 17 October 2005 earthquake seismic sequence in the Gulf of Sigacik (Seferihisar) along the Greek-Turkish borders. *Geophysical Research Abstracts*, 8, #08049.
- BRASIER, M.D., 1980. *Microfossils*. London: George Allen & Unwin.
- BRINKMANN, G., 1970. *Geology of Turkey*. New York: Elsevier Scientific.
- BRÜCKNER, H., 2003. Delta evolution and culture: Aspects of geoarchaeological research in Miletos and Priene. In: WAGNER, G.; PERINICKA, E., and UERPMANN, H.P. (eds.), *Troia and the Troad: Scientific Approaches*. Heidelberg, Germany: Springer-Verlag, pp. 121–142.
- CANN, J.H.; HARVEY, N.; BARNETT, E.J.; BELPERIO, A.P., and BOURMAN, R.P., 2002. Foraminiferal biofacies eco-succession and Holocene sealevels, Port Pirie, South Australia. *Marine Micropaleontology*, 44(1), 31–55.
- CIMMERMAN, F. and LANGER, M.R., 1991. Mediterranean foraminifera. Slovenian Academy of Sciences and Arts, Natural History, vol. 30. Paleontologica Institute Ivana Rakovca 2: Ljubljana.
- CROUCH, D.P.; BRÜCKNER, H.; KRAFT, J.; ORTLOFF, C., and VETTERS, W., 2002. Urban design amid flooding and sedimentation: the case of Ephesus. International Commission on Irrigation and Drainage, 18th Congress (Montreal, Quebec).
- CURRAY, J.R.; EMMEL, F.J., and CRAMPTON, P.J.S., 1969. Holocene history of a strand plain, lagoonal coast, Nayarit, Mexico. In CASTANARES, F.B. (ed.), *Coastal Lagoons: A Symposium*. Mexico City: Universidad Nacional Autonoma, pp. 63–100.
- CURREY, D., 1966. Problems of correlation in the Anglo-Paris-Belgian basin. *Proceedings of the Geological Association*, 77, 437–465.
- DALRYMPLE, R.W.; ZAITLIN, B.A., and BOYD, R., 1992. Estuarine facies models: conceptual basis and stratigraphic implications. *Journal of Sedimentary Petrology*, 62, 1130–1146.
- ERKANAL, H., 1995. 1993 Liman Tepe Kazıları. *Kazı Sonuçları Toplantısı*, 16, 263–279 [in Turkish].
- EROL, O., 1981. Neotectonic and geomorphological evolution of Turkey. *Zeitschrift für Geomorphologie, Neue Folge*, 40 (Supplement), 193–211.
- FIEST-CASTEL, M., 1977. Evolution of the charophyte floras in the upper Eocene and lower Oligocene of the Isle of Wight. *Palaeontology*, 20, 143–157.
- FIORINI, F., 2004. Benthic foraminiferal associations from Upper Quaternary deposits of southeastern Po Plain, Italy. *Micropaleontology*, 50, 1, 45–58.
- FISHBEIN, E. and PATTERSON, R.T., 1993. Error weighted maximum likelihood, EWML: a new statistically based method to cluster quantitative micropaleontological data. *Journal of Paleontology*, 67, 475–486.
- FLEMMING, N.C., 1978. Holocene eustatic changes and coastal tectonics in the northeast Mediterranean: implications for models of crustal consumption. *Philosophical Transactions of the Royal Society of London*, 289(1362), 405–458.
- FOUACHE, E.; SIBELLA, P., and DALONGEVILLE, R., 1999. Holocene variations of the shoreline between Antalya and Andriake, Turkey. *International Journal of Nautical Archaeology*, 28(4), 305–318.
- GACIA, E. and DUARTE, C.M., 2001. Sediment retention by a Mediterranean *Posidonia oceanica* meadow: the balance between deposition and resuspension. *Estuarine, Coastal and Shelf Science*, 52, 505–514.
- HAMMER, O.; HARPER, D., and RYAN, P.D., 2001. PAST: paleontological statistics software package for education and data analysis. *Palaeontologia Electronica*, 4(1), 1–9.
- HAYWARD, B.W.; HOLZMANN, M.; GRENFELL, H.R.; PAWLOWSKI, J., and TRIGGS, C.M., 2004. Morphological distinction of molecular types in *Ammonia*: towards a taxonomic revision of the world's most commonly misidentified foraminifera. *Marine Micropaleontology*, 50, 237–271.
- HEISSERER, A.J., 1980. *Alexander the Great and the Greeks*. Norman, Oklahoma: University of Oklahoma Press.
- HOTTINGER, L.; HALICZ, E.; REISS, Z., and DROBNE, K., 2003. *Recent Foraminiferida from the Gulf of Aqaba, Red Sea*. Ljubljana, Slovenia: Slovenian Academy of Sciences and Arts and the Swiss Academy of Natural Sciences.
- HYAMS, O.; ALMOGI-LABIN, A., and BENJAMINI, C., 2002. Larger foraminifera of the southeastern Mediterranean shallow continental shelf off Israel. *Israel Journal of Earth Sciences*, 51, 169–179.
- KAYAN, I., 1988. Late Holocene sea-level changes on the western Anatolian coast. *Palaeogeography, Palaeoclimatology, Palaeoecology*, 68(2–4), 205–218.
- KRAFT, J.C. and RAPP, G.J., 1975. Late Holocene paleogeography of the coastal plain of the Gulf of Messenia, Greece, and its relationships to archaeological settings and coastal change. *Geological Society of America Bulletin*, 86, 1191–1208.
- KRAFT, J.C.; ASCHENBRENNER, S.E., and RAPP, G.J., 1977. Paleogeographic reconstructions of coastal Aegean archaeological sites. *Science*, 195, 941–947.
- KRAFT, J.C.; KAYAN, I., and EROL, O., 1980. Geomorphic reconstructions in the environs of Ancient Troy. *Science*, 209, 776–782.
- KRAFT, J.C.; RAPP, G.; KAYAN, I., and LUCE, J.V., 2003. Harbor ar-

- neas at ancient Troy: sedimentology and geomorphology complement Homer's Iliad. *Geology*, 31(2), 163–166.
- LAMBECK, K., 1996. Sea-level change and shoreline evolution in Aegean Greece since Upper Paleolithic time. *Antiquity*, 70, 588–613.
- LAMBECK, K. and BARD, E., 2000. Sea-level change along the French Mediterranean coast for the past 30,000 years. *Earth and Planetary Science Letters*, 175, 203–222.
- LAMBECK, K. and PURCELL, A., 2005. Sea-level change in the Mediterranean Sea since the LGM: model predictions for tectonically stable areas. *Quaternary Science Reviews*, 24, 1969–1988.
- LAMBECK, K.; FABRIZIO, A.; PURCELL, A., and SILENZI, S., 2004. Sea-level change along the French Mediterranean coast for the past 30,000 years. *Earth and Planetary Science Letters*, 175, 203–222.
- LESSA, G. and MASSELINK, G., 2006. Evidence of a mid-Holocene sea-level highstand from the sedimentary record of a macrotidal barrier and paleoestuary system in Northwestern Australia. *Journal of Coastal Research*, 22, 100–112.
- MURRAY, J., 1991. *Ecology and Palaeoecology of Benthic Foraminifera*. New York: John Wiley & Sons.
- NICHOLS, G., 1999. *Sedimentology and Stratigraphy*. Oxford: Blackwell Science.
- NIXON, C., 2001. Foraminifera, tidal notches, and neotectonic events in Greece. Hamilton, Ontario: McMaster University, unpublished Master's thesis.
- NUR, A. and CLINE, E.H., 2000. Poseidon's horses: plate tectonics and earthquake storms in the later Bronze Age Aegean and Eastern Mediterranean. *Journal of Archaeological Science*, 27, 43–63.
- PAPAZACHOS, B.C.; COMNINAKIS, P.E.; KARAKAISIS, G.F.; KARAKOSTAS, B.G.; PAPAIOANNOU, CH.A.; PAPAZACHOS, C.B., and SCORDILIS, E.M., 2000. *A Catalogue of Earthquakes in Greece and Surrounding Area for the Period 550 BC–1999*. Thessaloniki: Publication Geophysics Laboratory, University of Thessaloniki.
- PIRAZOLLI, P.A., 1994. Tectonic Shorelines. In: CARTER, R.W. and WOODROFFE, C.W. (eds.), *Coastal Evolution: Late Quaternary Shoreline Morphodynamics*. Cambridge, UK: Cambridge University Press, pp. 451–476.
- REINHARDT, E.; FITTON, R., and SCHWARCZ, H., 2003. Isotopic (Sr, O, C) indicators of salinity and taphonomy in marginal marine systems. *Journal of Foraminiferal Research*, 33(3), 262–272.
- RUIZ, F.; GONZALEZ-REGALADO, M.L.; PENDON, J.G.; ABAD, M.; OLIAS, M., and MUNOZ, J.M., 2005. Correlation between foraminifera and sedimentary environments in recent estuaries of southwestern Spain: applications to Holocene reconstructions. *Quaternary International*, 140–141, 21–36.
- SAMIR, A.M.; ABDOU, H.F.; ZAZOU, S.M., and EL-MENHAWAY, W.H., 2003. Cluster analysis of recent benthic foraminifera from the northwestern Mediterranean coast of Egypt. *Revue de Micropaleontology*, 46, 111–130.
- SANER, E., 1994. *A 3-Dimensional Model for Coastal and Estuarine Waters Embedded in a PC-Based IDE*. Izmir, Turkey: Dokuz Eylül University.
- SAYIN, E., 2003. Physical features of the Izmir Bay. *Continental Shelf Research*, 23, 957–970.
- SCOTT, D.B. and MEDIOLI, F.S., 1978. Vertical zonations of marsh foraminifera as accurate indicators of former sea levels. *Nature*, 272, 528–531.
- SCOTT, D.B. and MEDIOLI, F.S., 1986. Foraminifera as sea-level indicators. In: VAN DE PLESSCHE, O. (ed.), *Sea-Level Research: A Manual for the Collection and Evaluation of Data*. Norwich: Geo Books, pp. 435–456.
- SCOTT, D.B.; SCHAFER, C., and MEDIOLI, F.S., 2001. *Monitoring in Coastal Environments Using Foraminifera and Thecomobian Indicators*. Cambridge, UK: Cambridge University Press, 192p.
- SHORT, A.D., 1988. The South Australia coast and Holocene sea-level transgression. *Geographical Review*, 78(2), 119–136.
- SIVAN, D.; ELIYAHU, D., and RABAN, A., 2004. Late Pleistocene to Holocene wetlands now covered by sand, along the Carmel Coast, Israel, and their relation to human settlement: an example from Dor. *Journal of Coastal Research*, 20(4), 1035–1048.
- SIVAN, D.; YECHIELI, Y.; HERUT, B., and LAZAR, B., 2005. Geochemical evolution and timescale of seawater intrusion into the coastal aquifer of Israel. *Geochimica et Cosmochimica Acta*, 69(3), 579–592.
- SOULIÉ-MÄRSCHKE, I., 1991. Charophytes as lacustrine biomarkers during the Quaternary in North Africa. *Journal of African Earth Sciences*, 12, 341–351.
- TESSON, M.; LABAUNE, C., and GENSOUS, B., 2005. Small rivers contribution to the Quaternary evolution of a Mediterranean littoral system: the western gulf of Lion, France. *Marine Geology*, 222–223, 313–334.
- VANICEK, V.; JURACIC, M.; BAJRAKTAREVIC, Z., and COSOVIC, V., 2000. Benthic foraminiferal assemblages in a restricted environment: an example from the Mljet Lakes, Adriatic Sea, Croatia. *Geology of Croatia*, 53(2), 269–279.
- VELLA, C. and PROVENSAL, M., 2000. Relative sea-level rise and neotectonic events during the last 6500 yr on the southeastern Rhône Delta, France. *Marine Geology*, 170, 27–39.
- VÖTT, A.; BRUCKNER, H.; SCHRIEVER, A.; LUTHER, J.; HANDLE, M., and VAN DER BORG, K., 2006. Holocene paleogeographies of the Palairos coastal plain (Akarnania, northwest Greece) and their geoarchaeological implications. *Geoarchaeology*, 21(7), 649–664.
- WALKER, R.G. and PLINT, A.G., 1992. *Wave- and Storm-Dominated Shallow Marine Systems. In Facies Models: Response to Sea Level Change*, pp. 219–238. Newfoundland: Geological Association of Canada.
- ZATON, M.; PIECHOTA, A., and SIENKIEWICZ, E., 2005. Late Triassic charophytes around the bone-bearing bed at Krasiejów, SW Poland: palaeoecological and environmental remarks. *Acta Geologica Polonica*, 55(3), 283–293.

Copyright of Journal of Coastal Research is the property of Allen Press Publishing Services Inc. and its content may not be copied or emailed to multiple sites or posted to a listserv without the copyright holder's express written permission. However, users may print, download, or email articles for individual use.